





Molecular Phylogenetics and Evolution

Volume 127, October 2018, Pages 168-178

New insights on the phylogenetic relationships among the traditional *Philodendron* subgenera and the other groups of the *Homalomena* clade (Araceae)

Santelmo Vasconcelos ^{a b}  , [Maria de Lourdes Soares ^c](#), [Cássia M. Sakuragui ^d](#), [Thomas B. Croat ^e](#), [Guilherme Oliveira ^a](#), [Ana M. Benko-Iseppon ^f](#)

Show more 

 Outline |  Share  Cite

<https://doi.org/10.1016/j.ympev.2018.05.017> ↗

[Get rights and content](#) ↗

Under an Elsevier [user license](#) ↗

open access

Highlights

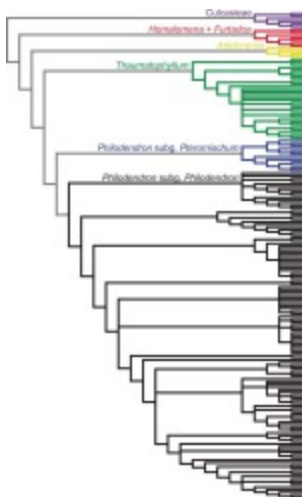
- *Philodendron sensu lato* is a monophyletic group.
- The three main morphologic lineages of *Philodendron s.l.* are monophyletic.
- *Thaumatophyllum* is the first diverging lineage of the group.
- *P.* subg. *Pteromischum* is a well-defined group with high statistical support.
- There are three major distinct lineages in *P.* subg. *Philodendron*.

- The genus *Homalomena* is not monophyletic without the species of *Furtadoa*.

Abstract

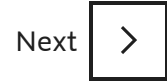
Philodendron (Araceae) is one of the largest Neotropical plant genera, with approximately 500 species and at least 1000 species predicted. There is a considerable ecological diversity in the group, although most species occur in the humid forests of tropical America. Despite being relatively well-studied in taxonomic analyses, the relationships among the traditional morphological groups of the genus are not well-established, mainly regarding the three traditional subgenera, referred here as *Philodendron sensu lato* (*s.l.*), *P.* subg. *Pteromischum*, *P.* subg. *Philodendron* and *P.* subg. *Meconostigma*, which was recently recognized as a separate genus, *Thaumatophyllum*. Therefore, the present work evaluates the phylogenetic position and the monophyly of *Philodendron s.l.* and its three main subdivisions, and the sister groups within the *Homalomena* clade, which also includes the Neotropical genus *Adelonema*, the two Asian genera *Homalomena* and *Furtadoa*, and the two African genera *Cercestis* and *Culcasia*, by means of molecular phylogenetic approaches including chloroplast DNA (*atpF-atpH*, *rpl32-trnL*, *trnQ-5'-rps16* and *trnV-ndhC*) and nuclear (ITS2) markers. The monophyly of *Philodendron s.l.* and its three lineages is confirmed and our analyses corroborate previous morphologic data indicating *Thaumatophyllum* as sister to the clade formed by *P.* subg. *Pteromischum* and *P.* subg. *Philodendron*.

Graphical abstract



[Download: Download high-res image \(77KB\)](#)

[Download: Download full-size image](#)



Keywords

Adelonema; Aroideae; *Homalomena* clade; *Meconostigma*; *Pteromischum*; *Thaumatophyllum*

1. Introduction

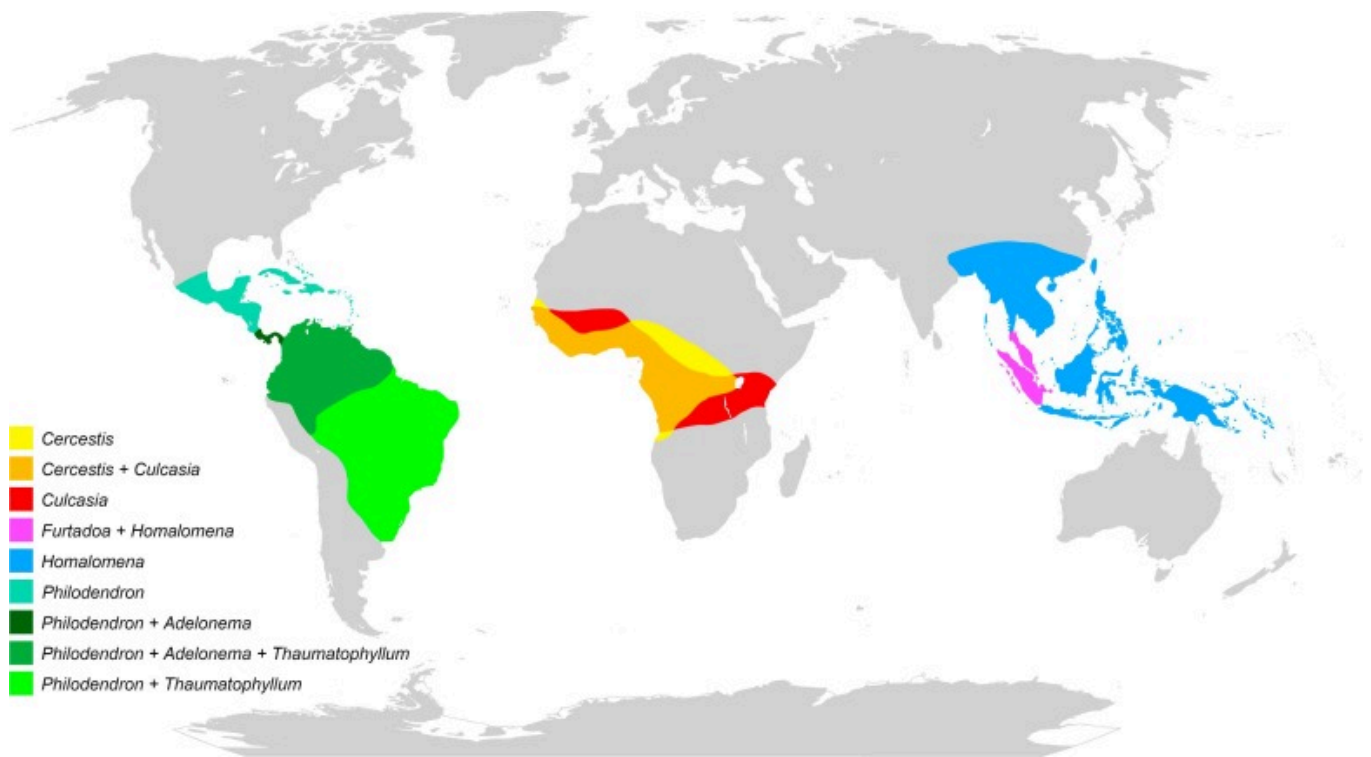
Philodendron Schott is one of the largest Neotropical plant taxa, being the second most species-rich genus within *Araceae*, with approximately 500 described species, but at least 1000 predicted ([The Plant List, 2013](#), [Boyce and Croat, 2018](#)). The group presents considerable morphological and ecological diversities ([Fig. 1](#)), occurring mainly in the humid forests of tropical America ([Mayo, 1988](#), [Mayo, 1991](#), [Mayo et al., 1997](#)), with a considerable geographic distribution ranging from Mexico to Uruguay ([Mayo et al., 1997](#)). Additionally, due to the remarkable abundance of the species of *Philodendron* in their respective environments, the genus is regarded as one of the most important epiphytic components of the Neotropical flora (see [Gentry and Dodson, 1987](#), [Croat, 1997](#), [Irumé et al., 2013](#)). Although there is evidence that the geographic origin of *Philodendron* is placed in the Amazon basin ([Calazans et al., 2014](#), [Loss-Oliveira et al., 2016](#)), the biogeographic history of the major group in which the genus is inserted, the *Homalomena* clade *sensu* [Cusimano et al. \(2011\)](#), remains obscure. The *Homalomena* clade is composed of the *Philodendron* clade, which contains four genera (two from Tropical America, *Philodendron s.l.* and *Adelonema* Schott, and two from Southeastern Asia, *Homalomena* Schott, and *Furtadoa* M.Hotta) and the Culcasieae (with two genera from Central Africa – *Cercestis* Schott and *Culcasia* P.Beauv.) ([Fig. 2](#)).



[Download: Download high-res image \(1MB\)](#)

[Download: Download full-size image](#)

Fig. 1. Representing members of the three lineages of *Philodendron* *s.l.* in their respective habitats. *Thaumatococcus*: *T. corcovadense* (A), *T. spruceanum* (B) and *T. solimoense* (C); *P.* subg. *Philodendron*: *P. bipennifolium* (D), *P. callosum* (E), *P. distantilobum* (F), *P. linnaei* (G) and *P. megalophyllum* (H); and *P.* subg. *Pteromischum*: *P. rudgeanum* (I).



[Download: Download high-res image \(296KB\)](#)

[Download: Download full-size image](#)

Fig. 2. Geographic distribution of the seven genera of the *Homalomena* clade *sensu* Cusimano et al. (2011), based on Mayo, 1991, Mayo et al., 1997.

Philodendron s.l. is composed of three major morphological groups: (1) *Philodendron* subgenus *Meconostigma* (Schott) Engler (21 spp. endemic to South America), recently recognized as the separate genus *Thaumatophyllum* Schott by Sakuragui et al. (2018), constituted mainly of arborescent heliophytes, although with some species adapted to shady environments; (2) *Philodendron* subgenus *Pteromischum* (Schott) Mayo (78 spp.), constituted mainly of lianescent species from Central America and Northern South America, although some species occur in Eastern and Central South America; and (3) *Philodendron* subgenus *Philodendron* Engler (ca. 400 spp.), by far the most morphologically diverse group, although the nomadic vine habit (according to Zotz, 2013) is presented by most of the species, being distributed through the whole geographic range of the genus. The subgenus *Philodendron* is subdivided into 10 morphological sections: *Baursia* (Rchb. ex Schott) Engler, *Camptogynium* K.Krause, *Dolichogynium* Croat and Köster, *Macrobelyium* (Schott) Sakur., *Macrogynium* Engler, *Philodendron* (Jacq.) Schott, *Philopsammos* G.S.Bunting, *Polytomium* (Schott) Engler, *Schizophyllum* (Schott) Engler and *Tritomophyllum* (Schott) Engler. However, most of these groups may be artificial, as suggested by Croat (1997) and indicated by previous molecular phylogenetic analyses (Gauthier et al., 2008, Loss-Oliveira et al., 2016),

considering that the diagnostic morphologic characters for such sections are potentially homoplastic.

In addition to the relatively recent taxonomic treatments for some of these morphologic groups of the genus, such as [Mayo, 1991](#), [Gonçalves and Salviani, 2002](#) for *Thaumatophyllum* (as *P.* subg. *Meconostigma*), [Grayum \(1996\)](#) for *P.* subg. *Pteromischum* from Pacific and Caribbean tropical America, [Croat \(1997\)](#) for *P.* subg. *Philodendron* from Mexico and Central America, [Sakuragui et al. \(2005\)](#) for *P.* sect. *Macrobelum* from Brazil, [Sakuragui \(2012\)](#) for *P.* sect. *Schizophyllum* and [Barbosa and Sakuragui \(2014\)](#) for extra-Amazonian species of *P.* subg. *Pteromischum*, there are some molecular phylogenies focusing on both inter- and intrageneric relationships of *Philodendron* ([Gauthier et al., 2008](#), [Wong et al., 2013](#), [Wong et al., 2016](#), [Loss-Oliveira et al., 2016](#)). According to the analyses by [Gauthier et al., 2008](#), [Wong et al., 2013](#), [Wong et al., 2016](#)), there is an indication that *Philodendron s.l.* may not be monophyletic, since the relationships between species of *P.* subg. *Pteromischum* and *Adelonema*, a genus that until recently was recognized as the American portion of the genus *Homalomena* (*Homalomena* sect. *Curmeria*), were not well-resolved. On the other hand, [Loss-Oliveira et al. \(2016\)](#) observed the analyzed species of *P.* subg. *Pteromischum* appearing within subgenus *Philodendron*, besides the relative difficulty of recovering the whole genus *Philodendron* as monophyletic. However, one may take notice of the appreciably small sampling of *P.* subg. *Pteromischum* in all these studies, where just two species were included by [Gauthier et al., 2008](#), [Wong et al., 2013](#), [Wong et al., 2016](#)) and three by [Loss-Oliveira et al. \(2016\)](#).

Therefore, the present analysis aimed a better resolution of the phylogenetic relationships within *Philodendron s.l.* with a more comprehensive sampling among the genera *Philodendron sensu stricto* (*s.s.*) (*P.* subg. *Pteromischum* and *P.* subg. *Philodendron*), *Thaumatophyllum* and the sister groups from the *Homalomena* clade, taking into account a molecular phylogeny analysis based on four intergenic chloroplast markers (*atpF-atpH*, *rpl32-trnL*, *trnQ-5'-rps16* and *trnV-ndhC*) and the nuclear marker ITS2.

2. Materials and methods

2.1. Plant material and DNA extraction

The DNA extractions were performed from 196 accessions of 151 species of the *Homalomena* clade, including 111 species of *Philodendron s.s.* (ca. 23% of the genus), 18 of *Thaumatophyllum* (ca. 86%) six of *Adelonema*, nine of *Homalomena*, one of *Furtadoa*, one of *Cercestis* and three of *Culcasia*. Fresh young leaves were sampled from individuals of both

natural populations and living collections, as indicated in Table S2. For the plants from field collections, leaves were stored in a NaCl-saturated solution of 2% CTAB (Rogstad, 1992). DNA extraction procedures followed the CTAB I protocol, as described by Weising et al. (2005) with an additional step of polysaccharide precipitation, as described by Michaels et al. (1994).

2.2. DNA amplification and sequencing

The chloroplast markers *rpl32-trnL*, *trnV-ndhC* and *trnQ-5'-rps16* were amplified by using the primers described by Shaw et al. (2007), while for the *atpF-atpH* region, we used the primer set employed by Fazekas et al. (2008). For the amplification of the nuclear ITS2, we used the primers S2F and S3R described by Chen et al. (2010). All PCRs were conducted as follows: initial denaturation for 3 min at 94 °C, followed by 30 cycles of 1 min at 94 °C, 1 min at 54 °C and 1 min at 72 °C, with a final extension step for 7 min at 72 °C, in a 25 µL reaction containing ~10–100 ng of genomic DNA, 1 × *Taq* buffer with KCl (Thermo Scientific), 3 µmol/mL MgCl₂ (Thermo Scientific), 0.2 µmol/mL of each dNTP, 0.1 nmol/mL of each primer and 1 U of *Taq* DNA polymerase (Thermo Scientific). In the case of the ITS2 reactions, 2 µL of dimethyl sulfoxide (DMSO) were added to the PCR mixture.

Bidirectional sequencing reactions were performed with the BigDye Terminator v3.1 Cycle Sequencing kit (Applied Biosystems) and were analyzed either in an ABI PRISM 3500 Genetic Analyzer (Applied Biosystems) or in a ABI 3730 DNA Analyzer (Applied Biosystems). The resulting sequencing reads were assembled and edited with Geneious R11 (Biomatters Ltd.) and then separately aligned for each region with MAFFT 7.017 (Kato and Standley, 2013) using the algorithm *Auto*, with minor manual corrections. For the analysis of the ITS2 region, we also used previously published ITS sequences of species of *Philodendron s.l.*, *Adelonema*, *Homalomena* and *Furtadoa* (Gauthier et al., 2008, Wong et al., 2013, Wong et al., 2016), which were available in the NCBI database (Supplementary Table S1). Additionally, we tested the performance of the alignments with and without indel regions in the five markers.

2.3. Phylogenetic analyses

Dendrograms were generated for each region separately, as well as two concatenated analyses, one with the four chloroplast markers and one adding the ITS2 to the cpDNA regions (but using only the samples that were sequenced for all the five markers), using three different approaches – maximum parsimony (MP), maximum likelihood (ML) and Bayesian inference (BI). The search for the best-fit substitution model for each region was performed in jModelTest 2 (Darriba et al., 2012), based on both the Bayesian Information

Criterion (BIC) and the Decision Theory (DT) calculations, as suggested by the results of [Ripplinger and Sullivan, 2008](#), [Luo et al., 2010](#). The MP analyses were conducted in TNT v1.5 ([Goloboff et al., 2008](#)), setting the heuristic searches for a maximum of 10000 and 1000000 trees for the ITS2 and cpDNA regions, respectively, and tree-bisection-reconnection (TBR) branch swapping, using a bootstrap analysis with 1000 replicates. The ML approach was performed with RAxML 8.2.8 ([Stamatakis, 2014](#)) using the rapid bootstrapping option with 1000 replicates. Since the general time reversible model and its variants are the only available options in RAxML, we replaced the best-fit models observed in jModelTest by the GTR+ Γ . The BI analyses were performed in MrBayes 3.2 ([Ronquist et al., 2012](#)) using four simultaneous runs, each with four Markov chains (T=0.2). The analyses started with randomly chosen trees, being extended through 50000000 generations, with sampling every 5000 generations and using a burn-in fraction of 25% of the trees. The model selection, the ML and the BI analyses were performed as implemented in the CIPRES portal (<http://www.phylo.org> ↗).

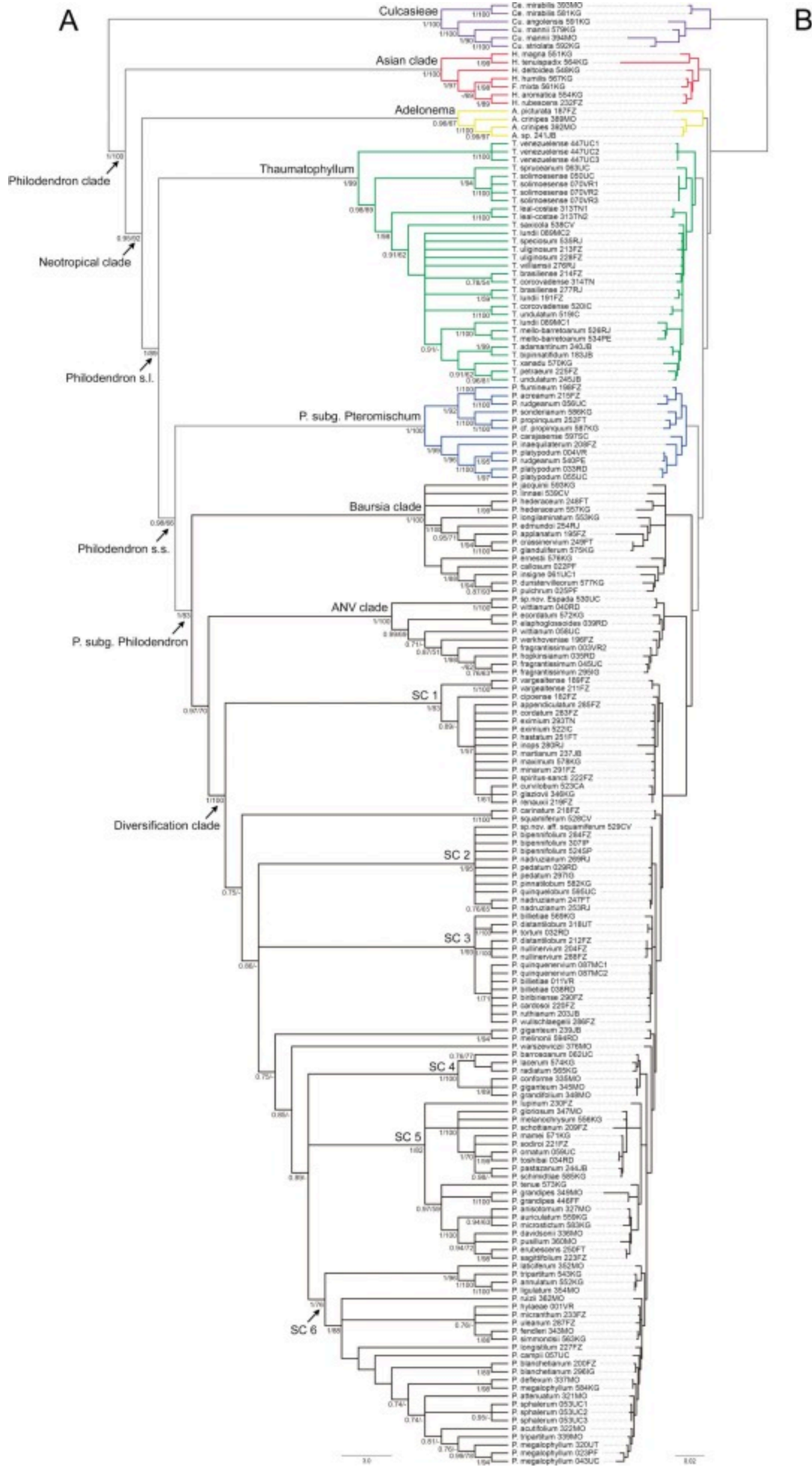
The topological congruence among the different partitions was tested using a Bayesian Concordance Analysis (BCA) performed in BUCKy 1.4.1 ([Ané et al., 2007](#), [Larget et al., 2010](#)), comparing all five regions. For each region, the resultant trees from the four MCMCMC chains were summarized, and then another 20% of the trees were removed as burn-in. The BCA was run with six a priori levels of discordance among loci ($\alpha=0.1, 0.5, 1, 5, 10$ and 100), using the options of four independent runs, four chains (three heated and one cold) and 10000000 generations. Additionally, an explorative network analysis using the NeighborNet algorithm implemented in Splitstree v.4.14 ([Huson and Bryant, 2006](#)) was performed, to check for conflicting phylogenetic signals within the data of all constructed matrixes.

3. Results

Sequences of the five used regions were obtained for the 196 accessions (135 spp.) of the ingroup (containing the American portion of the *Homalomena* clade – *Adelonema* spp. and *Philodendron s.l.* spp.), 10 spp. of the sister group (Asian portion of the *Homalomena* clade – *Furtadoa* and *Homalomena* spp.) and four spp. of the outgroup (African portion of the *Homalomena* clade – *Cercestis* and *Culcasia* species), generating a concatenated matrix with 4570 bp, after the exclusion of the non-aligned ends. Considering all aligned regions separately, *atpF-atpH* presented 774 bp (ranging from 540 to 645 bp), *rpl32-trnL* 966 bp (634–709 bp), *trnQ-5'-rps16* 1687 bp (1061–1469 bp), *trnV-ndhC* 1141 bp (633–1040 bp) and ITS2 625 bp (291–539 bp).

3.1. Clusters and general topologies

The three different phylogenetic reconstruction methods resulted in similar topologies, both regarding the cpDNA ([Fig. 3](#) and [Supplementary Figs. S1–S4](#)) and the nuclear DNA markers ([Fig. 4](#)), especially considering the major groups (basal nodes). However, most support values in the MP were lower ([Supplementary Figs. S5–S7](#)), besides the higher number of unresolved branches, when comparing with the ML and BI analyses.



[Download: Download high-res image \(964KB\)](#)

[Download: Download full-size image](#)

Fig. 3. Majority-rule consensus tree (cladogram in A and phylogram in B) with species of the seven genera of the *Homalomena* clade based on Bayesian inference with the concatenated matrix of the chloroplast DNA markers *atpF-atpH*, *rpl32-trnL*, *trnQ-5'-rps16* and *trnV-ndhC*. Posterior probabilities (≥ 0.70) and bootstrap values (≥ 50), obtained from the maximum likelihood analysis with the same matrix, are indicated near the clade nodes.

[Download: Download full-size image](#)

Fig. 4. Majority-rule consensus tree (cladogram in A and phylogram in B) with species of the five genera of the *Philodendron* clade based on Bayesian inference with the nuclear rDNA ITS2 region. Posterior probabilities (≥ 0.70) and bootstrap values (≥ 50), obtained from the maximum likelihood analysis with the same matrix, are indicated near the clade nodes.

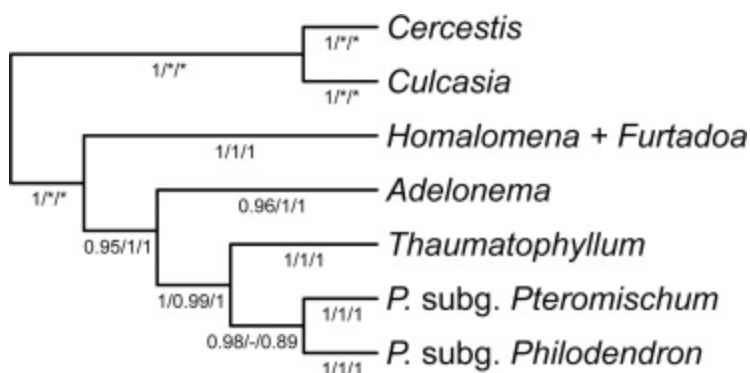
The concatenated analysis (cpDNA + ITS2) resulted in similar topologies for the three reconstruction methods, generally presenting good support values, mainly in the ML and the BI (Fig. 5). The separate analyses (i.e., independent runs with each marker) resulted mostly in unresolved basal and terminal nodes (Fig. 4 and Supplementary Figs. S1–S4), although the ITS2 was, by far, the best of the five used regions, showing a topology somewhat similar to the concatenated cpDNA analysis (Fig. 3). Therefore, from now on, only the ITS2, the cpDNA and the cpDNA + ITS2 trees will be mentioned in the text. Additionally, it is noteworthy that some of the species of *Thaumatophyllum* were recovered as monophyletic only in the ITS2 trees and not in the concatenated cpDNA trees (nor with the separate cpDNA regions).

[Download: Download high-res image \(1MB\)](#)

[Download: Download full-size image](#)

Fig. 5. Majority-rule consensus tree (cladogram in A and phylogram in B) with species of the five genera of the *Philodendron* clade based on Bayesian inference with the concatenated matrix of the chloroplast DNA markers *atpF-atpH*, *rpl32-trnL*, *trnQ-5'-rps16* and *trnV-ndhC* and the nuclear rDNA ITS2. Posterior probabilities (≥ 0.70) and bootstrap values (≥ 50), obtained from the maximum likelihood analysis with the same matrix, are indicated near the clade nodes. Abbreviations between parentheses after the species names correspond to the sectional affiliations, which were based on [Grayum, 1996](#), [Croat, 1997](#), [Sakuragui et al., 2005](#)., *P. sect. Boursia* (BA), *P. sect. Camptogynium* (CG), *P. sect. Fruticosa* (FR), *P. sect. Macrobelium* (MB), *P. sect. Macrogygium* (MG), *P. sect. Philodendron* (PD), *P. sect. Philopsammos* (PP), *P. sect. Polytomium* (PM), *P. sect. Pteromischum* (PT), *P. sect. Schizophyllum* (SZ) and *P. sect. Tritomophyllum* (TT).

In general, the basal nodes, which represent the main lineages of *Philodendron s.l.* (i.e., *Thaumatophyllum*, *P. subg. Pteromischum* and *P. subg. Philodendron*, and the three main clades of the last), as well as the other lineages of the *Homalomena* clade, were recovered with significant statistical support, mainly in the BI analyses ([Fig. 3](#), [Fig. 4](#), [Fig. 5](#), [Fig. 6](#)). However, it is important to note that due to the evolutionary distance among the sequences of the two African genera and the rest of the groups of the *Homalomena* clade ([Supplementary Fig. S8](#)), the ITS2 alignment contained only the Asian and the American lineages to avoid the excessive problems with homoplastic characters due to the fast-evolving nature of the region, which was hindering the tree reconstructions.



[Download: Download high-res image \(113KB\)](#)

[Download: Download full-size image](#)

Fig. 6. Summary tree of the major groups of the *Homalomena* clade, including the three lineages of *Philodendron s.l.*, showing posterior probability values of the cpDNA, ITS2 and

concatenated (cpDNA + ITS2) analyses, respectively, under the branches.

3.2. Relationships among the main lineages of the *Homalomena* clade

Only the African and the Neotropical groups of the *Homalomena* clade were recovered as monophyletic with good support values (Fig. 3, Fig. 4, Fig. 5, Fig. 6), whereas the species of *Furtadoa* were embedded in the genus *Homalomena*, where *F. mixta* and *F. sumatrensis* did not form a cohesive group in the ITS2 trees (the only analysis containing both species), appearing as independent lineages within the genus *Homalomena* (Fig. 4). On the other hand, considering the combination of the genera *Homalomena* + *Furtadoa*, the Asian clade presented the maximum support values (Fig. 3, Fig. 4, Fig. 5, Fig. 6).

As the *Culcasieae* species were used as outgroup in the cpDNA analyses, the first diverging lineage of the *Philodendron* clade was the Asian clade, which was divided into two and three main clades, in the cpDNA and ITS2 trees (depending on the number of sampled species), respectively, with good support values (Fig. 3, Fig. 4). In the ITS2 analysis, two sections of the genus *Homalomena*, *H. sect. Cyrtocladon* and *H. sect. Geniculatae*, were recovered with maximum posterior probabilities (PP) and good bootstrap (BS) values, but the species of *H. sect. Chamaecladon*, *H. sect. Homalomena* and *Furtadoa* were placed in a larger polyphyletic group with good statistical support (Fig. 4 and Supplementary Fig. S6). In the cpDNA and the concatenated analysis, the species of *H. sect. Cyrtocladon* were not sampled, although we observed a similar subdivision structure among the remaining sections of the genus *Homalomena* (Fig. 3, Fig. 5).

In almost all reconstruction methods, *Adelonema* was recovered as a monophyletic group, sister to the genus *Philodendron* with good support values, except for the ML and MP analyses with the cpDNA matrix, which presented BS of 67 and 60, respectively (Fig. 3 and Supplementary Fig. S5). Species of both sections of *Adelonema*, *A. sect. Adelonema* (PP=1, ML-BS=100 and MP-BS=100) and *A. sect. Curmeria* (PP=0.81, ML-BS=72 and MP-BS=86, respectively), were sampled only in the ITS2 analyses, being resolved as monophyletic, whereas the cpDNA trees only contained species of the last group (Fig. 3, Fig. 4).

The monophyly of the genus *Philodendron s.l.* was recovered with good statistical support in most of the analyses, especially in the BI trees (Fig. 3, Fig. 4, Fig. 5, Fig. 6). Within this group, all the three main lineages appeared as monophyletic with maximum PP values and good BS support (Fig. 3, Fig. 4, Fig. 5, Fig. 6). All the concatenated analyses and the cpDNA BI tree showed *Thaumatophyllum* as the first diverging lineage of *Philodendron s.l.* with significant support, thus grouping *P. subg. Pteromischum* and *P. subg. Philodendron* as sister clades, referred here as *Philodendron s.s.* (Fig. 3, Fig. 5). However, when both the cpDNA and ITS2

matrixes were run separately under the ML and MP approaches, the relationships among *Thaumatophyllum* and the two *Philodendron* subgenera were not clear, resulting either in the grouping of *Philodendron* s.s. with low support or in a polytomy (Fig. 3, Fig. 4; Supplementary Figs. S5–S7).

3.3. Relationships within *Philodendron* s.l.

Thaumatophyllum (*Philodendron* subg. *Meconostigma*). In both the cpDNA and the concatenated analyses, *T. venezuelense* appeared as the first diverging lineage within the genus and the other two Amazonian species of the group, *T. spruceanum* and *T. solimoesense*, formed a strongly supported group that was placed as sister to the species from the Eastern portion of South America (Fig. 3, Fig. 5). Within the Eastern species clade, which was recovered as monophyletic with strong statistical support, *T. leal-costae* was the first diverging species, whereas the remaining lineages of the group formed another clade with strong support values (Fig. 3, Fig. 5). On the other hand, the relationships among the four main lineages of *Thaumatophyllum* (*T. venezuelense*, *T. spruceanum*+*T. solimoesense*, *T. leal-costae* and the Eastern species clade) were not resolved in the ITS2 analyses (Fig. 4). It is important to notice that within the Eastern species clade the relationships among the species are unclear and most of the species with more than one sampled accession appeared as polyphyletic, mainly in the cpDNA trees, although some of these species were monophyletic in the ITS2 trees, such as *T. lundii* and *T. mello-barretoanum* (Fig. 3, Fig. 4, Fig. 5).

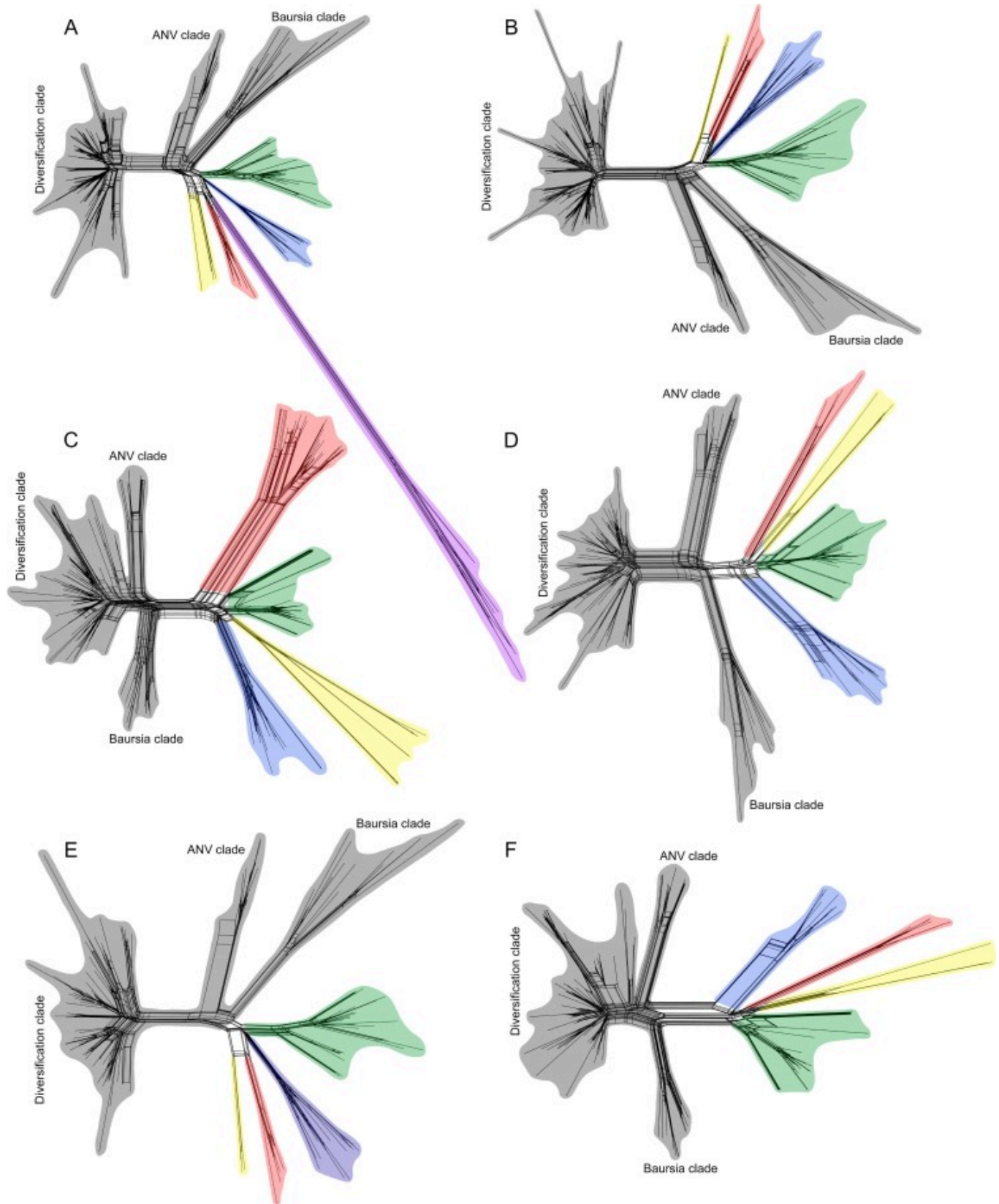
Philodendron subg. *Pteromischum*. None of the two sections (*P. sect. Fruticosa* and *P. sect. Pteromischum*) were recovered as monophyletic. However, in contrast to the other two subgenera of *Philodendron*, interspecific relationships among the sampled species *P. subg. Pteromischum* were mostly well-supported and well-resolved in all phylogenetic reconstructions (Fig. 3, Fig. 4, Fig. 5). As observed for other groups within the genus, some species were shown as polyphyletic (e.g., *P. rudgeanum* Schott) with high statistical support (Fig. 3, Fig. 4, Fig. 5).

Philodendron subg. *Philodendron*. The subgenus was divided into three main clades, with strong support in all reconstruction approaches: (A) the *Baursia* clade, which is the first diverging lineage within *P. subg. Philodendron* (Fig. 3, Fig. 4, Fig. 5), composed mostly of species from *P. sect. Baursia* and *P. sect. Philopsammos*, although some species from other sections, such as *P. hederaceum* (*P. sect. Philodendron*) and *P. jacquini* (*P. sect. Macrogynium*) grouped within this clade (Fig. 3, Fig. 4, Fig. 5); (B) the Amazon nomadic vines (or ANV) clade, which consists of species without a morphologic pattern (both in vegetative and floral characters), although with a similar habit and occurring in the Amazon basin – within this

clade, both *P. fragrantissimum* and *P. hopkinsianum* share a very similar habit, consisting of plants with relatively long internodes in the non-flowering portion and turning into a rosette with very short internodes in the flowering portion, grouping with high statistical support (Fig. 3, Fig. 4, Fig. 5); and (C) the diversification clade, by far the largest of the three main groups of *P. subg. Philodendron*, being subdivided in, at least, six recognizable subclades (SC 1–6) with strong PP values (Fig. 3, Fig. 5), with the SC 2 standing out the as the group formed by almost all sampled species of *P. sect. Schizophyllum* (Fig. 3, Fig. 4, Fig. 5). In addition, several species of *P. subg. Philodendron* with more than one sampled accession were not recovered as monophyletic, such as *P. billietiae*, *P. fragrantissimum* and *P. quinquenervium* (Fig. 3, Fig. 4, Fig. 5).

3.4. Congruence among partitions and phylogenetic networks

As observed in the phylogenetic trees, the eight major groups within the *Homalomena* clade (Culcasieae, Asian clade, *Adelonema*, *Thaumatophyllum*, *P. subg. Pteromischum*, *Baursia* clade, ANV clade and the diversification clade) were recovered in all phylogenetic networks, considering the six used data matrixes: (1) full cpDNA; (2) full cpDNA without Culcasieae; (3) full ITS2; (4) concatenated (cpDNA+ITS2); (5) reduced cpDNA and (6) reduced ITS2, both only with the species of the concatenated matrix (Fig. 7). However, the order of the splits varied among the six different networks, from which, only the concatenated analysis (cpDNA+ITS2) showed similar relationships as those shown in the phylogenetic trees (Fig. 7 D). In general, although the major groups could be easily identified in the phylogenetic networks, the splits within and among the groups were somewhat inconsistent, mainly in the case of *P. subg. Philodendron* and of the Asian clade (Fig. 7; Supplementary Fig. S9). In addition, within *P. subg. Philodendron*, as observed in the phylogenetic trees, the *Baursia* and ANV clades were positioned as more closely related to the other lineages of the *Homalomena* clade than to the diversification clade in all analyses using cpDNA data (Fig. 7 A,B, D–F).



[Download: Download high-res image \(1MB\)](#)

[Download: Download full-size image](#)

Fig. 7. NeighborNet splits based on the uncorrected p-distance with the groups of the *Homalomena* clade (A) and *Philodendron* clade (B-F), using six different matrixes:

concatenated cpDNA markers (A); concatenated cpDNA without *Culcasieae* (B); ITS2 (C); concatenated cpDNA and ITS2 (D); reduced cpDNA (E) and reduced ITS2 (F). The colors represent the major groups of the *Homalomena* clade: *Philodendron* subg. *Philodendron* in grey, which was subdivided into three independent clusters (1 – diversification clade, 2 – ANV clade, and 3 – *Baursia* clade), *P.* subg. *Pteromischum* in blue, *Thaumatophyllum* in green, *Adelonema* in yellow, the Asian clade (*Homalomena* and *Furtadoa*) in red and the *Culcasieae* (*Cercestis* + *Culcasia*) in purple.

4. Discussion

The species of *Philodendron s.l.* have a pronounced presence in Neotropical humid forests, being the main components of the epiphytic flora of some regions (e.g. [Irumé et al., 2013](#)). Nevertheless, the phylogenetic relationships among most of the morphological subdivisions of the group are still unresolved, especially regarding the traditional recognition of three subgenera. Despite the first cladistics approach with *Philodendron s.l.* being developed more than 30 years ago, employing both vegetative and reproductive morphological characters ([Mayo, 1986](#)), several questions concerning the infrageneric circumscriptions remained unaddressed two decades later, until the first large-scale molecular phylogenetic analysis by [Gauthier et al. \(2008\)](#), using the cpDNA marker *rpl16* and the nuclear loci ETS and ITS. In fact, the available data at that time could neither validate nor refute the morphologic groups within *Philodendron s.l.*, due to low statistical support values and conflicting topologies, depending on the used phylogenetic reconstruction method. The authors even questioned the monophyly of the genus as it was circumscribed at the time, considering that the relationships between the American species of *Homalomena* (now circumscribed in the recently resurrected *Adelonema*) and the subgenera of *Philodendron* (especially *P.* subg. *Pteromischum*) were unclear, as mentioned before ([Gauthier et al., 2008](#), [Wong et al., 2013](#), [Wong et al., 2016](#)).

In the more recent analysis by [Loss-Oliveira et al. \(2016\)](#), *Philodendron s.l.* was not recovered as a monophyletic group with significant statistical support once more. It is important to notice that the authors used a supertree approach instead of a single matrix with all 116 sampled species (110 *Philodendron s.l.* spp. and 16 *Homalomena* spp., including *Adelonema*), which presented marked differences in sequencing success with each of the five regions, with the variation in species coverage ranging from 30 (*3' matK + trnK* intron) to 92 (*trnL-trnF*). On the other hand, except for the members of *P.* subg. *Pteromischum*, which appeared among species of *P.* subg. *Philodendron*, the main clades we observed within *Philodendron s.l.* were also recovered in the supertree by [Loss-Oliveira et al. \(2016\)](#). Therefore, the superior resolution we obtained here is probably associated with the higher species coverage with

the markers we employed, thus allowing the reconstruction of phylogenetic trees based on supermatrix analyses (180 species in the combined cpDNA tree and 143 species in the concatenated cpDNA+ITS2 tree), instead of the supertree approach as in [Loss-Oliveira et al. \(2016\)](#), as previously tested by [Janies et al. \(2013\)](#).

Another important aspect, which may also be related to the higher resolution we obtained in comparison to the previous phylogenetic analyses with *Philodendron s.l.*, is the high polymorphism levels of the markers used here, especially in the case of ITS2. In fact, [Gauthier et al., 2008](#), [Wong et al., 2013](#), [Wong et al., 2016](#)) already indicated the great potential of using the ITS marker (comprising the ITS1, 5,8S rDNA and ITS2 regions) when studying the phylogenetic relationships within the *Homalomena* clade. Even considering that we used only the ITS2 portion, basically due to multiple loci amplification in several *Philodendron s.l.* species when using the complete ITS marker ([Supplementary Fig. S10](#)), as widely described for plants ([Álvarez and Wendel, 2003](#), [Feliner and Rosselló, 2007](#)), the polymorphism observed here for the region was highly informative for our phylogenetic analysis. Similarly, all four cpDNA markers employed here, which also are non-coding regions, performed very well in the phylogenetic reconstructions, but only when put together in a single matrix, since none of the regions alone resulted in resolved trees ([Supplementary Figs. S1–S4](#)), as well as in the previous analyses with *Philodendron s.l.* ([Gauthier et al., 2008](#), [Loss-Oliveira et al., 2016](#)). Furthermore, it is important to indicate that indel regions were kept in the alignments of all five used markers, since their exclusion lowered the resolution of the phylogenetic trees ([Supplementary Figs. S11 and S12](#)), as previously reported by [Nagy et al. \(2012\)](#) for alignments based on ITS, which was caused by a higher conservation degree of indels rather than substitutions.

Our data validate, to a certain extent, the traditional morphologic groups within *Philodendron*. For the first time in a molecular phylogenetics approach, *Philodendron s.l.* was recovered as strongly monophyletic with all the three main morphological subdivisions (the three traditional subgenera) as independent lineages within the group. Also, *Thaumatophyllum* appears as sister to the two subgenera of *Philodendron s.s.* with strong support in the cpDNA and the concatenated trees, as observed with morphologic data by [Mayo \(1986\)](#). It is noteworthy that the presence of lobed styles in all *Thaumatophyllum* species, as well as in *Homalomena s.l.* (*Homalomena* + *Adelonema*), appears to be a plesiomorphic character within the *Philodendron* clade. These results contrast with the topologies presented by [Gauthier et al. \(2008\)](#) using two nuclear DNA markers (ETS and ITS), although with low support values, in which *P. subg. Pteromischum* was the first diverging lineage of *Philodendron s.l.*

Attempting to group the members of the highly diverse *P.* subg. *Philodendron*, which presents approximately four times more species than the junction of the other two main clades of *Philodendron s.l.*, several authors recognized 10 different sections based on morphologic characters ([Mayo, 1990](#), [Croat, 1997](#), [Sakuragui et al., 2005](#), [Köster and Croat, 2011](#)), from which the two largest, sections *Macrobelyium* and *Philodendron*, are subdivided into several subsections and series. However, none of the nine sampled sections of the subgenus were recovered as monophyletic (only the section *Dolychogynium*, which comprises two species, *P. delinksii* Croat and Koster and *P. sparreorum* Croat, was not sampled in this work), as indicated by the previous data ([Gauthier et al., 2008](#), [Loss-Oliveira et al., 2016](#)). Even the two monotypic sections *Camptogynium* (with *P. longistilum*) and *Macrogynium* (*P. jacquinii*) were not recovered as independent lineages, grouping within the diversification clade and the *Baursia* clade, respectively. These results indicate the weak nature of the morphologic characters that were used to delimitate the sections, such as in the case of *P. sect. Macrobelyium* and *P. sect. Philodendron*, which present a very high degree of morphologic variation, being defined only by the low and high number of ovules per locule, respectively. Also, the indication that the section *Tritomophyllum* (defined by the three-lobed leaves of its species, and here represented by *P. anisotomum*, *P. barrosoanum*, *P. hylaeae* and *P. tripartitum*) could be an artificial group ([Croat, 1997](#)) was confirmed here. The only section relatively well-defined is *P. sect. Schizophyllum*, from which almost all specimens formed a cohesive group with high statistical support, indicating that the morphological delimitation of the group is relatively well-defined ([Sakuragui, 2012](#)), although *P. ruthianum* Nadrusz was not recovered among the other members of the clade.

Regarding the clustering within *Thaumatophyllum*, the position of *T. venezuelense* as sister to the remaining species of the genus (in the cpDNA and concatenated analyses) contrasts with the topology presented by [Oliveira et al., 2014](#), [Sakuragui et al., 2018](#) with different markers. Instead, [Oliveira et al. \(2014\)](#) observed the clade formed by *T. spruceanum* (as *P. goeldii*) and *T. solimoesense* (as *P. solimoesense*) as the first diverging lineage of *Thaumatophyllum* (as *P.* subg. *Meconostigma*), besides the clustering of *T. venezuelense* (as *P. venezuelense*) within the heliophytes clade, as sister to *T. williamsii* (as *P. williamsii*), similarly to the results obtained by [Calazans et al. \(2014\)](#) in a phylogenetic analysis based on the morphology of reproductive characters. However, it is important to notice the robustness of our results towards the cohesion of the heliophytes clade without any of the Amazonian species, mainly regarding the cpDNA and concatenated matrixes, also containing *T. williamsii* (which is the same sample used by [Oliveira et al., 2014](#)), besides including three different specimens of *T. venezuelense*. Hence, we favor the hypothesis of a basal position of *T. venezuelense* within *Meconostigma*, as well as the other two species from the Amazon

basin (*T. spruceanum* and *T. solimoense*), a very likely scenario, according to the previously published ancestral biome reconstruction for *Philodendron* s.l. (Loss-Oliveira et al., 2016). In addition, one may consider that there was a single colonization event in the eastern portion of South America by the ancestral species of the genus, being a key factor during the diversification of *Thaumatophyllum*, as well as for the species of *P.* subg. *Philodendron*, as previously suggested (Calazans et al., 2014, Oliveira et al., 2014, Loss-Oliveira et al., 2016).

In the recent work by Wong et al. (2016), the American portion of the genus *Homalomena*, *H.* sect. *Curmeria*, was resurrected as the genus *Adelonema*, since the species from the Asian sections of the former genus and the two species of *Furtadoa* formed a clearly independent lineage. Moreover, the relationships among *Adelonema* and the remaining American lineages of the *Homalomena* clade are still unresolved, due to sampling issues, regarding the number of included species, in all the phylogenetic analyses covering the group so far, especially in the case of the species of *P.* subg. *Pteromischum*, which either appeared as sister to *Adelonema* (Gauthier et al., 2008, Wong et al., 2013, Wong et al., 2016) or as polyphyletic within *P.* subg. *Philodendron* (Gauthier et al., 2008, Loss-Oliveira et al., 2016). Nevertheless, our results show a clear monophyly of *Pteromischum* in all the approaches we tested, either in the conventional phylogenetic trees or in the phylogenetic networks. Besides, the group formed by the species of *Pteromischum* was recovered as sister to *P.* subg. *Philodendron* with strong support (cpDNA and concatenated matrixes), instead of being the first diverging lineage of *Philodendron* s.l., which was one of the suggested scenarios by Gauthier et al. (2008).

The separation of *Meconostigma* from the genus *Philodendron*, thus resurrecting the genus *Thaumatophyllum*, as recently proposed by Sakuragui et al. (2018), may also imply in the separation of *Pteromischum* from the genus *Philodendron*. Although the inclusion of *Adelonema* into *Philodendron* as its fourth subgenus, and thus the maintenance of *Meconostigma* and *Pteromischum* as subgenera, would demand less profound taxonomic changes, it is important to notice that our phylogenetic trees and networks indicate that *P.* subg. *Philodendron* is the more distantly related clade among the Neotropical lineages of the *Homalomena* clade. Moreover, *Adelonema*, *Thaumatophyllum*, *Pteromischum* and *P.* subg. *Philodendron* are groups easily distinguishable from one another, considering both morphological and ecological traits (Grayum, 1996, Croat, 1997, Mayo et al., 1997, Wong et al., 2016, Sakuragui et al., 2018). Hence, we suggest the resurrection of the genus *Elopium* Schott to encompass the species of *Pteromischum*, which is consistent with the previous decisions of separating *H.* sect. *Curmeria* into *Adelonema* (Wong et al., 2016) and *P.* subg. *Meconostigma* into *Thaumatophyllum* (Sakuragui et al., 2018).

Declarations of interest

None.

Acknowledgements

This work was supported by CAPES (Coordenação de Aperfeiçoamento de Pessoal de Nível Superior), CNPq (Conselho Nacional de Desenvolvimento Científico e Tecnológico), FACEPE (Fundação de Amparo à Ciência e Tecnologia de Pernambuco) and Vale. We would like to thank to Emily Colletti, Dr. Mônica M. Carlsen and Dr. Elizabeth Kellogg for the samples obtained from the Araceae living collection of the Missouri Botanical Garden; to Dr. Felix Forest, Dr. Simon J. Mayo, Edith Kapinos and Marcelo Sellaro for the samples from the DNA bank and Araceae living collection the Royal Botanic Gardens, Kew (Richmond, Surrey, United Kingdom); to Dr. Eduardo G. Gonçalves and Ines Ribeiro for the samples from the living collection at the Fundação Zoobotânica de Belo Horizonte (Belo Horizonte, Minas Gerais, Brazil); to Dr. Marcus A. Nadruz Coelho for the samples from the Rio de Janeiro Botanical Garden; and to Dr. Heidi Cruz for the sequencing analyses with the ABI PRISM 3500 at the Universidade Federal de Pernambuco. AMBI, CMS and GO are CNPq fellows.

Appendix A. Supplementary material

[Download all supplementary files](#)

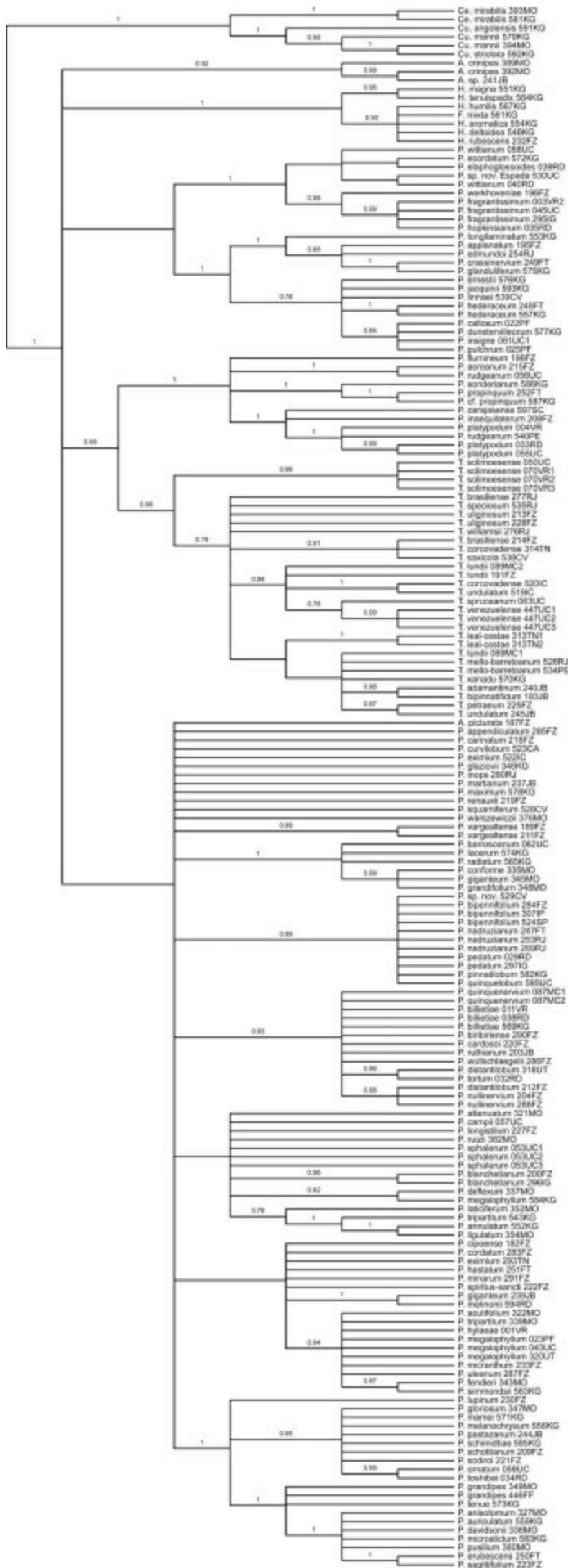
[? What's this? ↗](#)

The following are the Supplementary data to this article:

[Download: Download high-res image \(385KB\)](#)

[Download: Download full-size image](#)

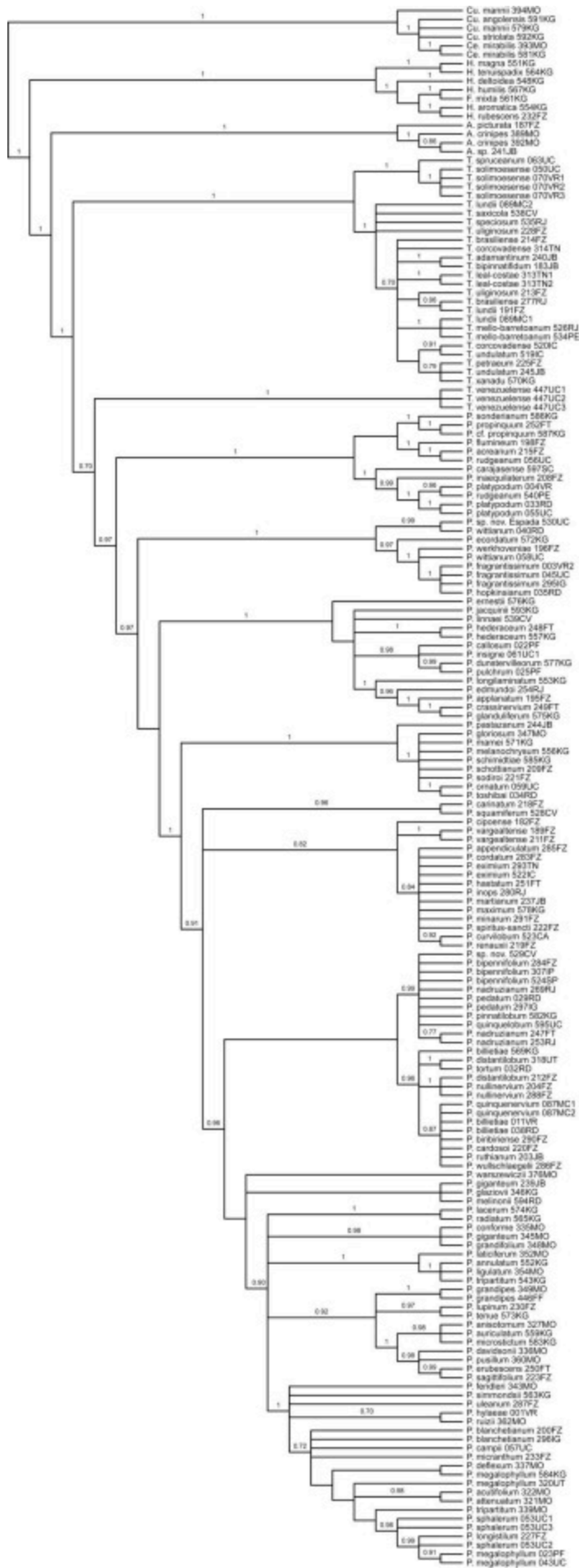
Supplementary figure 2. Majority-rule consensus tree with species of the seven genera of the Homalomena clade based on Bayesian inference with the chloroplast DNA marker *atpF-atpH*. Posterior probabilities (0.70) are indicated in the branches



[Download: Download high-res image \(363KB\)](#)

[Download: Download full-size image](#)

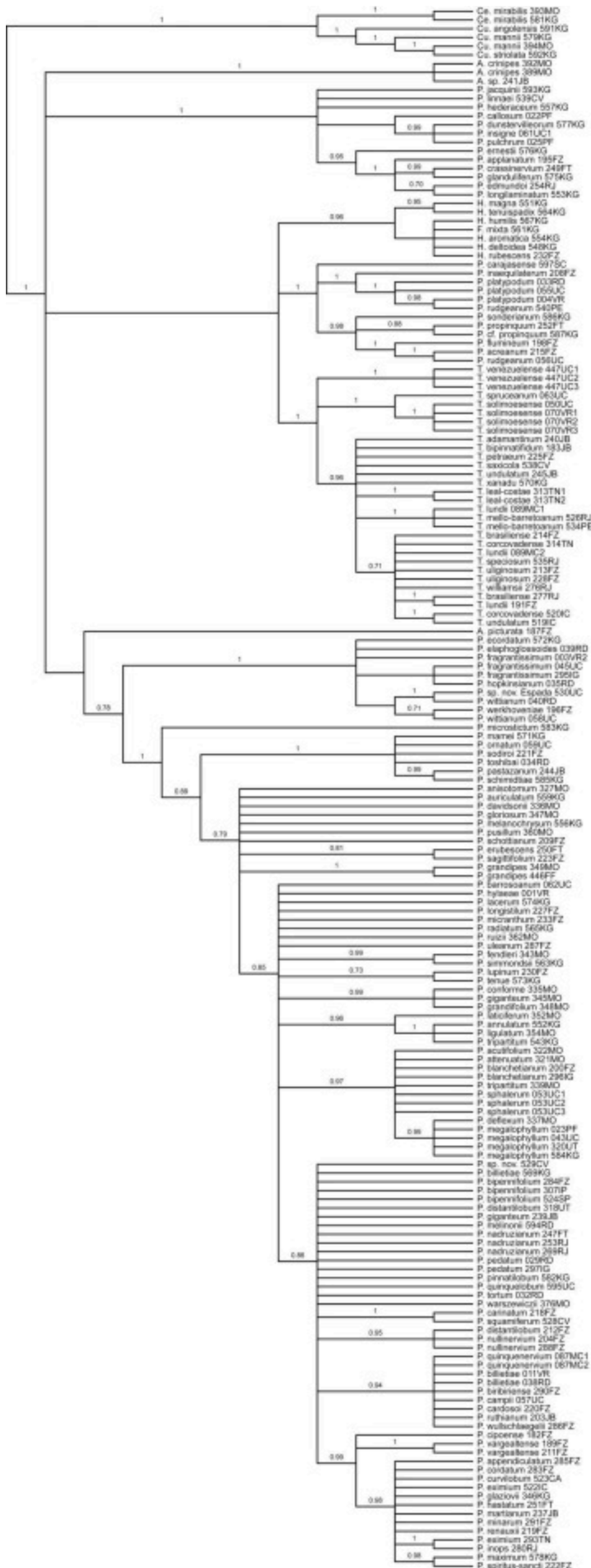
Supplementary figure 3. Majority-rule consensus tree with species of the seven genera of the *Homalomena* clade based on Bayesian inference with the chloroplast DNA marker *rpl32-trnL*. Posterior probabilities (0.70) are indicated in the branches



[Download: Download high-res image \(346KB\)](#)

[Download: Download full-size image](#)

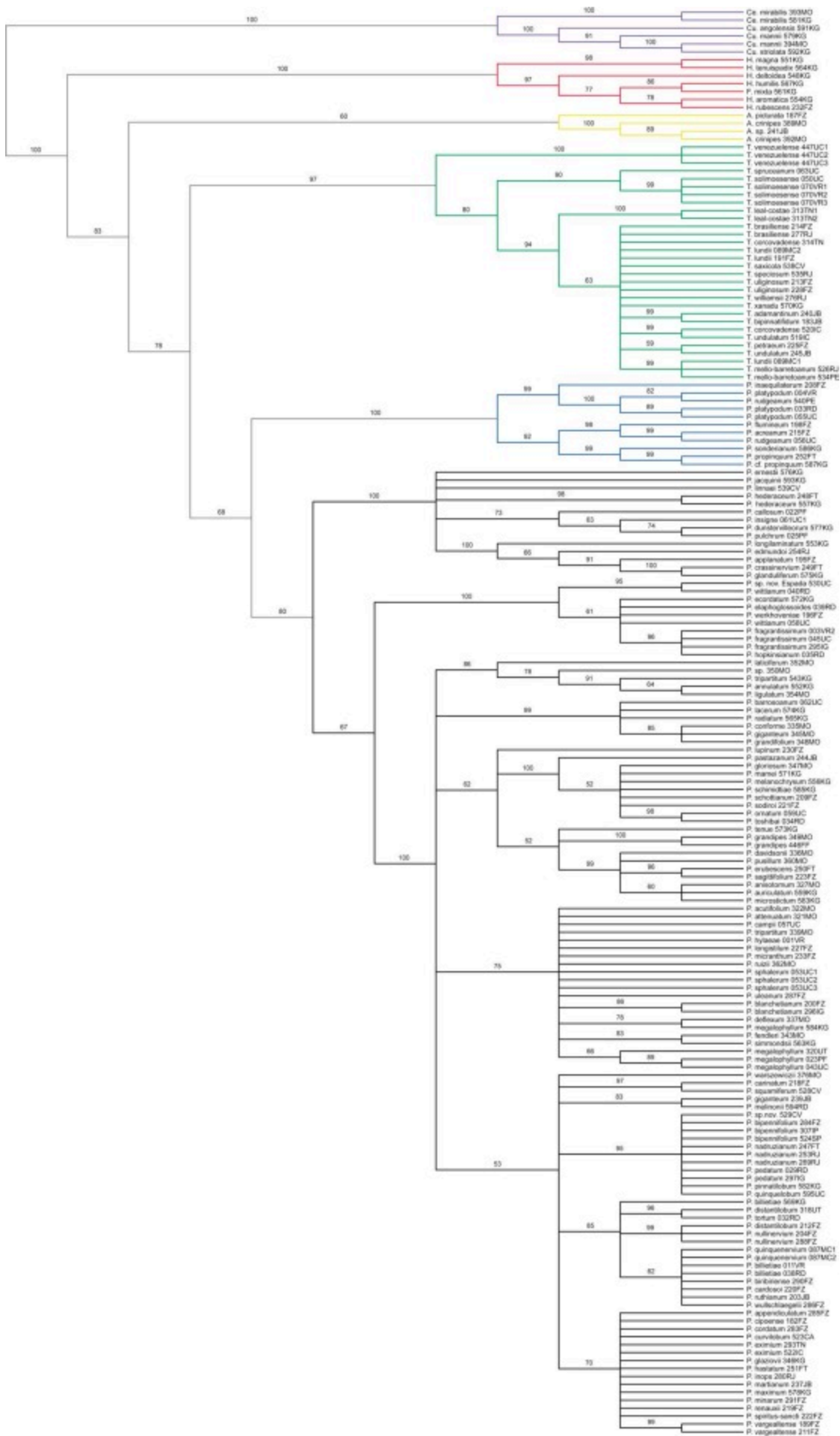
Supplementary figure 4. Majority-rule consensus tree with species of the seven genera of the Homalomena clade based on Bayesian inference with the chloroplast DNA marker trnQ-5'-rps16. Posterior probabilities (0.70) are indicated in the branches



[Download: Download high-res image \(367KB\)](#)

[Download: Download full-size image](#)

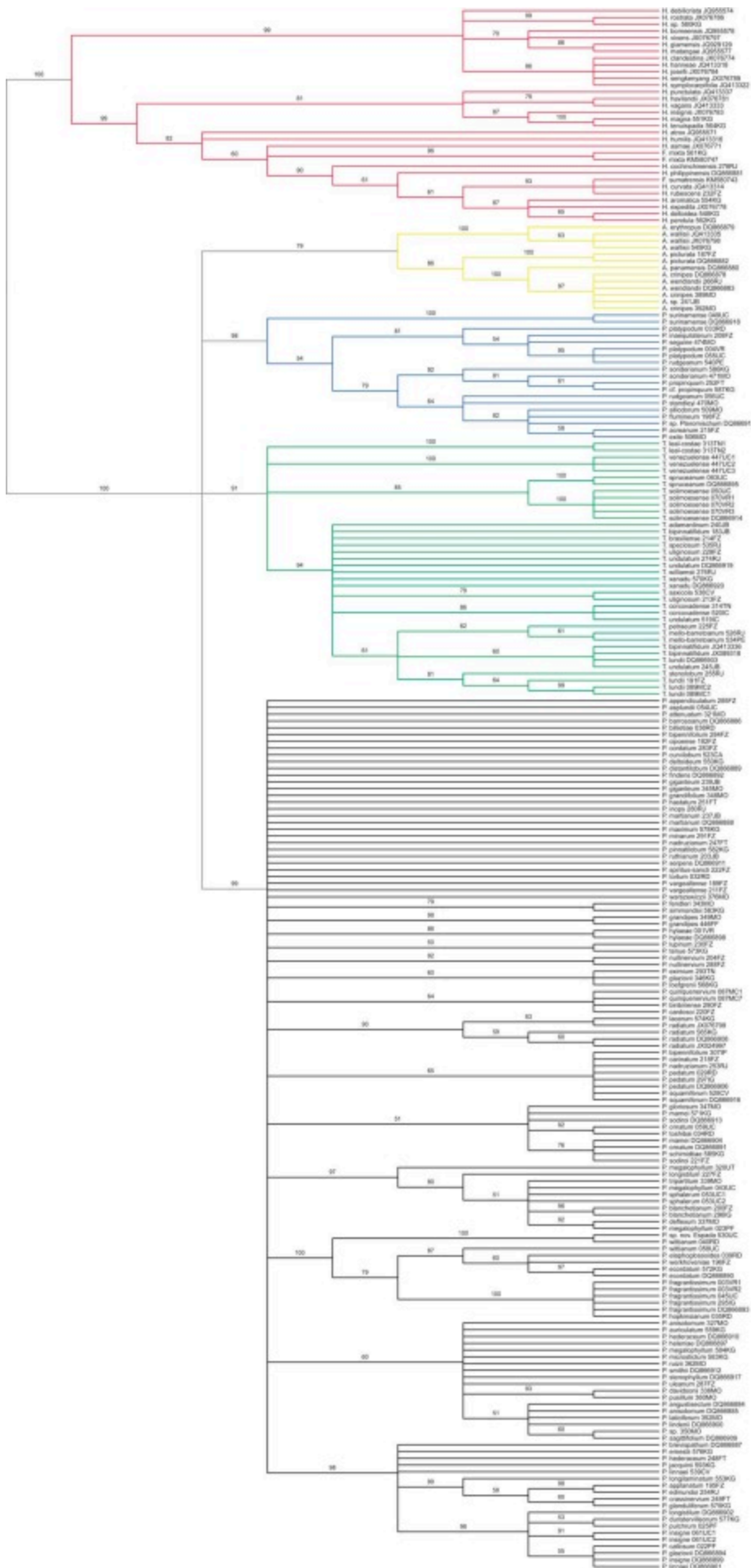
Supplementary figure 5. Majority-rule consensus tree with species of the seven genera of the Homalomena clade based on Bayesian inference with the chloroplast DNA marker trnV-ndhC. Posterior probabilities (0.70) are indicated in the branches



[Download: Download high-res image \(387KB\)](#)

[Download: Download full-size image](#)

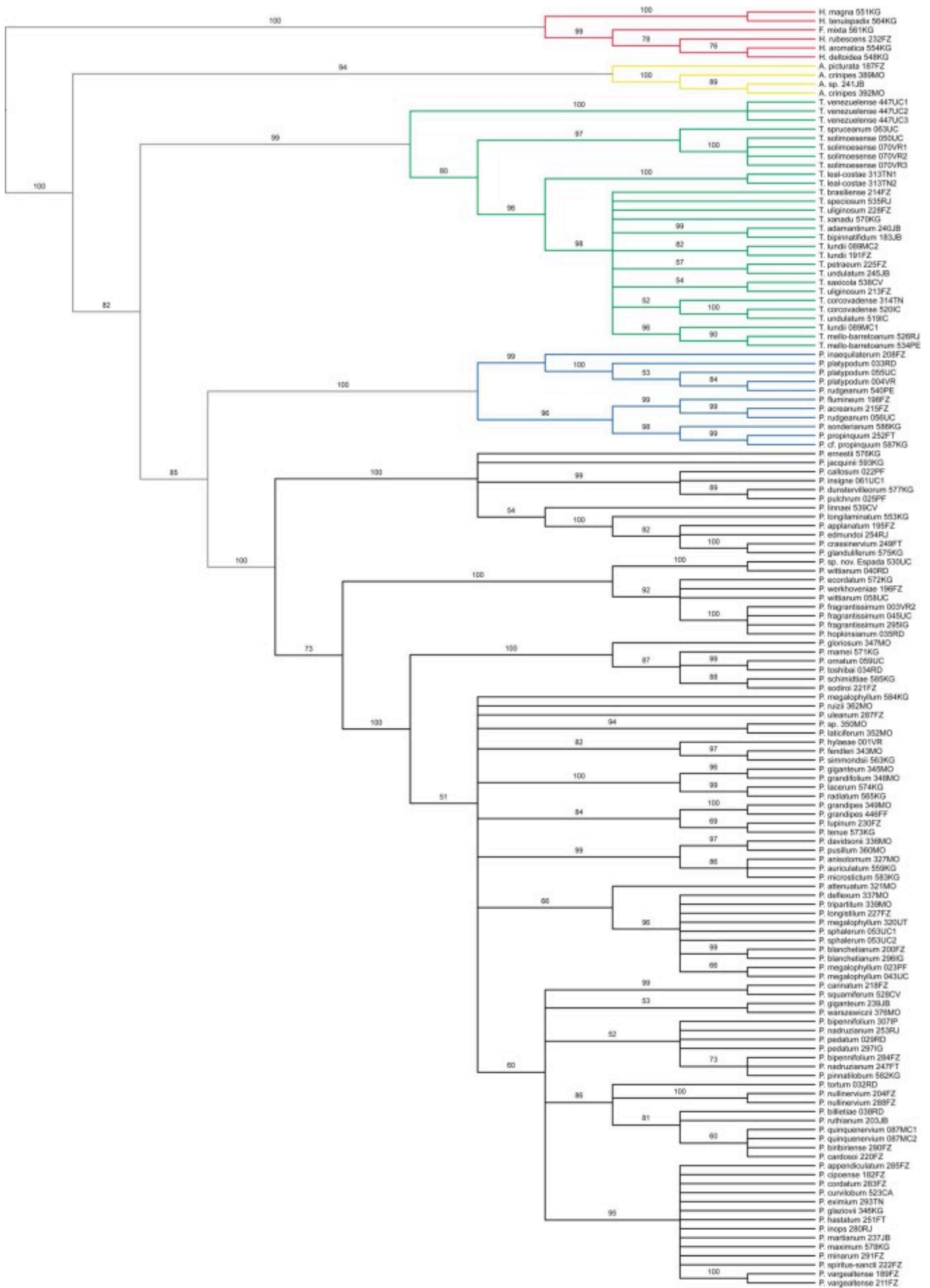
Supplementary figure 6. Majority-rule consensus tree analysis with species of the seven genera of the Homalomena clade based on the maximum parsimony analysis with the concatenated matrix of the chloroplast DNA markers *atpF-atpH*, *rpl32-trnL*, *trnQ-5'-rps16* and *trnV-ndhC*. Bootstrap values (50) are indicated in the branches. The colors represent the major groups of the Homalomena clade: *Philodendron* subg. *Philodendron* in grey, *P.* subg. *Pteromischum* in blue, *Thaumatococcus* in green, *Adelonema* in yellow, the Asian clade (*Homalomena* and *Furtadoa*) in red and the *Culcasieae* (*Cercestis* + *Culcasia*) in purple



[Download: Download high-res image \(407KB\)](#)

[Download: Download full-size image](#)

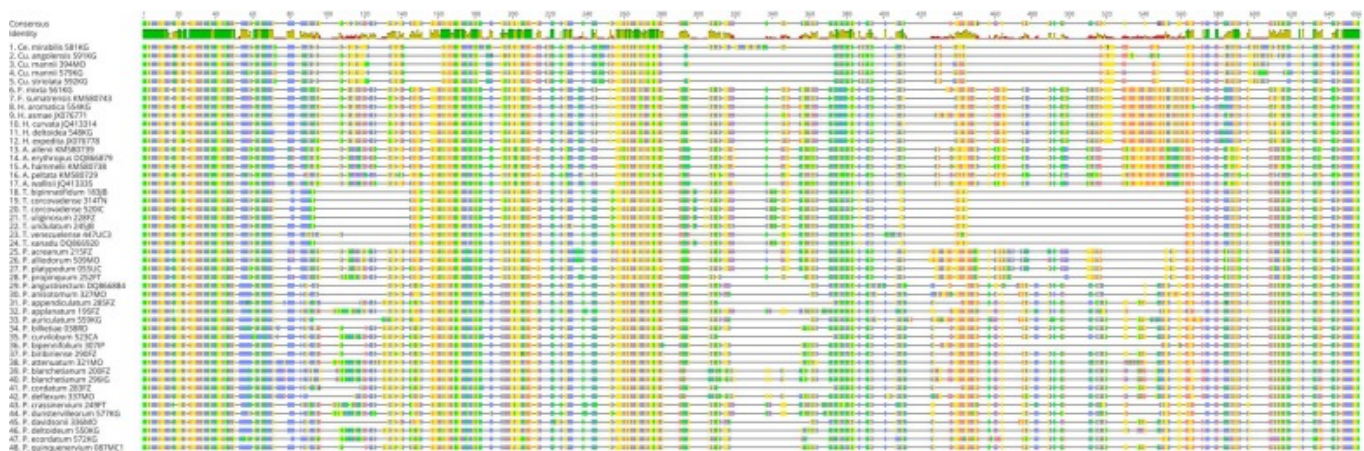
Supplementary figure 7. Majority-rule consensus tree analysis with species of the five genera of the *Philodendron* clade based on the maximum parsimony analysis with the nuclear rDNA ITS2 region. Bootstrap values (50) are indicated in the branches. The colors represent the major groups of the *Philodendron* clade: *Philodendron* subg. *Philodendron* in grey, *P.* subg. *Pteromischum* in blue, *Thaumatophyllum* in green, *Adelonema* in yellow and the Asian clade (*Homalomena* and *Furtadoa*) in red



[Download: Download high-res image \(440KB\)](#)

[Download: Download full-size image](#)

Supplementary figure 8. Majority-rule consensus tree with species of the five genera of the *Philodendron* clade based on the maximum parsimony analysis with the concatenated matrix of the chloroplast DNA markers *atpF-atpH*, *rpl32-trnL*, *trnQ-5'-rps16* and *trnV-ndhC* and the nuclear *rDNA ITS2*. Bootstrap values (50) are indicated in the branches. The colors represent the major groups of the *Philodendron* clade: *Philodendron* subg. *Philodendron* in grey, *P.* subg. *Pteromischem* in blue, *Thaumatophyllum* in green, *Adelonema* in yellow and the Asian clade (*Homalomena* and *Furtadoa*) in red

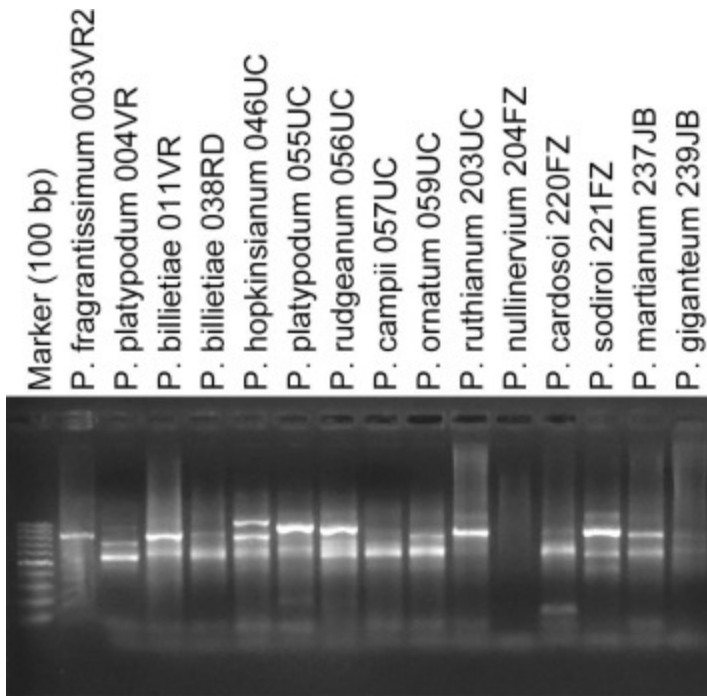


[Download: Download high-res image \(602KB\)](#)

[Download: Download full-size image](#)

Supplementary figure 9. ITS2 alignment with species of the Homalomena clade, including *Culcasieae* spp., showing the different distribution patterns of nucleotides and indels among the genera. The different colors represent the four nucleotides: A in red, T in green, C in blue and G in yellow

ANV clade, and 3 – *Baursia* clade), *P.* subg. *Pteromischum* in blue, *Thaumatophyllum* in green, *Adelonema* in yellow and the Asian clade (*Homalomena* and *Furtadoa*) in red



[Download: Download high-res image \(132KB\)](#)

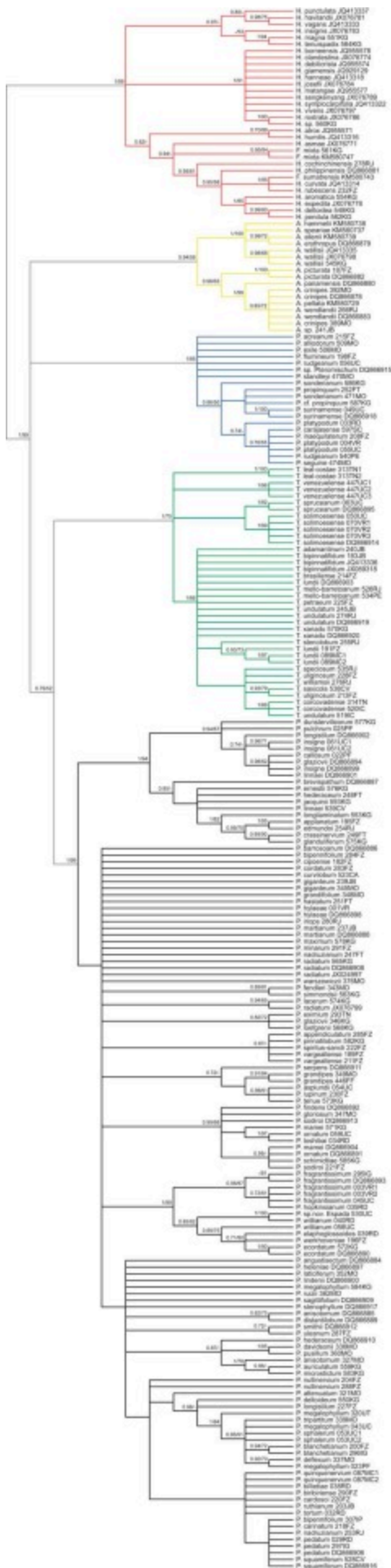
[Download: Download full-size image](#)

Supplementary figure 11. Electrophoresis gel showing the amplification pattern of the complete ITS marker (comprising the ITS1, 5.8S rDNA and ITS2 regions) from *Philodendron* spp. with the primers used by Gauthier et al. (2008), evidencing multiple amplified fragments in most of the used samples

[Download: Download high-res image \(339KB\)](#)

[Download: Download full-size image](#)

Supplementary figure 12. Majority-rule consensus tree with species of the seven genera of the Homalomena clade based on Bayesian inference with the concatenated matrix of the chloroplast DNA markers *atpF-atpH*, *rpl32-trnL*, *trnQ-5'-rps16* and *trnV-ndhC* excluding the indel regions. Posterior probabilities (0.70) and bootstrap values (50), obtained from the maximum likelihood analysis with the same matrix, are indicated near the clade nodes. The colors represent the major groups of the Homalomena clade: *Philodendron* subg. *Philodendron* in grey, *P.* subg. *Pteromischum* in blue, *Thaumatophyllum* in green, *Adelonema* in yellow, the Asian clade (*Homalomena* and *Furtadoa*) in red and the *Culcasieae* (*Cercestis* + *Culcasia*) in purple



[Download: Download high-res image \(312KB\)](#)

[Download: Download full-size image](#)

Supplementary figure 13. Majority-rule consensus tree with species of the five genera of the Philodendron clade based on Bayesian inference with the nuclear rDNA ITS2 region. Posterior probabilities (0.70) and bootstrap values (50), obtained from the maximum likelihood analysis with the same matrix, are indicated near the clade nodes. The colors represent the major groups of the Philodendron clade: Philodendron subg. Philodendron in grey, P. subg. Pteromischum in blue, Thaumatophyllum in green, Adelonema in yellow and the Asian clade (Homalomena and Furtadoa) in red

 [Download: Download Word document \(43KB\)](#)

Supplementary data 1.

 [Download: Download XML file \(258B\)](#)

Supplementary data 2.

[Recommended articles](#)

Research data for this article

 *Data not available / Data will be made available on request*

 [Further information on research data](#) ↗

References

[Álvarez and Wendel, 2003](#) I. Álvarez, J.F. Wendel
Ribosomal ITS sequences and plant phylogenetic inference
Mol. Phylogenet. Evol., 29 (2003), pp. 417-434
 [View PDF](#) [View article](#) [View in Scopus](#) ↗ [Google Scholar](#) ↗

[Ané et al., 2007](#) C. Ané, B. Larget, D.A. Baum, S.D. Smith, A. Rokas
Bayesian estimation of concordance among gene trees
Mol. Biol. Evol., 24 (2007), pp. 412-426

[View in Scopus ↗](#) [Google Scholar ↗](#)

[Barbosa and Sakuragui, 2014](#) J.F. Barbosa, C.M. Sakuragui

Taxonomy and conservation of the Brazilian extra-Amazonian species of *Philodendron* subg. *Pteromischum* (Araceae)

Phytotaxa, 191 (2014), pp. 45-65

[Crossref ↗](#) [View in Scopus ↗](#) [Google Scholar ↗](#)

[Boyce and Croat, 2018](#) Boyce, P.C., Croat, T.B., 2018. The Überlist of Araceae, totals for published and estimated number of species in aroid genera.

<http://www.aroid.org/genera/180211uberlist.pdf> ↗ (accessed 4 May 2018).

[Google Scholar ↗](#)

[Calazans et al., 2014](#) L.S.B. Calazans, C.M. Sakuragui, S.J. Mayo

From open areas to forests? The evolutionary history of *Philodendron* subgenus *Meconostigma* (Araceae) using morphological data

Flora, 209 (2014), pp. 117-121



[View PDF](#) [View article](#) [View in Scopus ↗](#) [Google Scholar ↗](#)

[Chen et al., 2010](#) S. Chen, H. Yao, J. Han, C. Liu, J. Song, L. Shi, Y. Zhu, X. Ma, T. Gao, X. Pang, K. Luo, Y. Li, X. Li, X. Jia, Y. Lin, C. Leon

Validation of the ITS2 region as a novel DNA barcode for identifying medicinal plant species

Plos One, 5 (2010), p. e8613

[Crossref ↗](#) [View in Scopus ↗](#) [Google Scholar ↗](#)

[Croat, 1997](#) T.B. Croat

A revision of *Philodendron* subgenus *Philodendron* (Araceae) for Mexico and Central America

Ann. Mo. Bot. Gard., 84 (1997), pp. 311-704

[Crossref ↗](#) [View in Scopus ↗](#) [Google Scholar ↗](#)

[Cusimano et al., 2011](#) N. Cusimano, J. Bogner, S.J. Mayo, P.C. Boyce, S.Y. Wong, M. Hesse, W.L.A. Hettterscheid, R.C. Keating, J.C. French

Relationships within the Araceae: comparison of morphological patterns with molecular phylogenies

Am. J. Bot., 98 (2011), pp. 654-668

[Crossref ↗](#) [View in Scopus ↗](#) [Google Scholar ↗](#)

[Darriba et al., 2012](#) D. Darriba, G.L. Taboada, R. Doallo, D. Posada

jModelTest 2: more models, new heuristics and parallel computing

Nat. Methods, 9 (2012), p. 772

[Crossref ↗](#) [View in Scopus ↗](#) [Google Scholar ↗](#)

[Fazekas et al., 2008](#) A.J. Fazekas, K.S. Burgess, P.R. Kesanakurti, S.W. Graham, S.G. Newmaster, B.C. Husband, D.M. Percy, M. Hajibabaei, S.C.H. Barrett

Multiple multilocus DNA barcodes from the plastid genome discriminate plant species equally well

Plos One, 3 (2008), p. e2802

[Crossref ↗](#) [View in Scopus ↗](#) [Google Scholar ↗](#)

[Feliner and Rosselló, 2007](#) G.N. Feliner, J.A. Rosselló

Better the devil you know? Guidelines for insightful utilization of nrDNA ITS in species-level evolutionary studies in plants

Mol. Phylogenet. Evol., 44 (2007), pp. 911-919

 [View PDF](#) [View article](#) [View in Scopus ↗](#) [Google Scholar ↗](#)

[Gauthier et al., 2008](#) M.P.L. Gauthier, D. Barabe, A. Bruneau

Molecular phylogeny of the genus *Philodendron* (Araceae): delimitation and infrageneric classification

Bot. J. Linn. Soc., 156 (2008), pp. 13-27

[Crossref ↗](#) [View in Scopus ↗](#) [Google Scholar ↗](#)

[Gentry and Dodson, 1987](#) A.H. Gentry, C.H. Dodson

Diversity and biogeography of Neotropical vascular epiphytes

Ann. Mo. Bot. Gard., 74 (1987), pp. 205-233

[Crossref ↗](#) [Google Scholar ↗](#)

[Goloboff et al., 2008](#) P.A. Goloboff, J.S. Farris, K.C. Nixon

TNT, a free program for phylogenetic analysis

Cladistics, 24 (2008), pp. 774-786

[Crossref ↗](#) [View in Scopus ↗](#) [Google Scholar ↗](#)

[Gonçalves and Salviani, 2002](#) E.G. Gonçalves, E.R. Salviani

New species and changing concepts of *Philodendron* subgenus *Meconostigma* (Araceae)

Aroideana, 25 (2002), pp. 2-15

[Google Scholar ↗](#)

[Grayum, 1996](#) M.H. Grayum

Revision of *Philodendron* subgenus *Pteromischum* (Araceae) for Pacific and Caribbean tropical America

Syst. Bot. Monogr., 47 (1996), pp. 1-233

[Crossref ↗](#) [Google Scholar ↗](#)

[Huson and Bryant, 2006](#) D.H. Huson, D. Bryant

Application of phylogenetic networks in evolutionary studies

Mol. Biol. Evol., 23 (2006), pp. 254-267

[Crossref ↗](#) [View in Scopus ↗](#) [Google Scholar ↗](#)

[Irumé et al., 2013](#) M.V. Irumé, M.L.C.S. Morais, C.E. Zartman, I.L. Amaral

Floristic composition and community structure of epiphytic angiosperms in a terra firme forest in central Amazonia

Acta Bot. Bras., 27 (2013), pp. 378-393

[View in Scopus ↗](#) [Google Scholar ↗](#)

[Janies et al., 2013](#) D.A. Janies, J. Studer, S.K. Handelman, G. Linchangco

A comparison of supermatrix and supertree methods for multilocus phylogenetics using organismal datasets

Cladistics, 29 (2013), pp. 560-566

[Crossref ↗](#) [View in Scopus ↗](#) [Google Scholar ↗](#)

[KatoH and Standley, 2013](#) K. KatoH, D.M. Standley

MAFFT multiple sequence alignment software version 7: improvements in performance and usability

Mol. Biol. Evol., 30 (2013), pp. 772-780

[Crossref ↗](#) [View in Scopus ↗](#) [Google Scholar ↗](#)

[Köster and Croat, 2011](#) N. Köster, T.B. Croat

A new section and a new species of *Philodendron* (Araceae) from Ecuador

Willdenowia, 41 (2011), pp. 119-124

[Crossref ↗](#) [View in Scopus ↗](#) [Google Scholar ↗](#)

[Larget et al., 2010](#) B.R. Larget, S.K. Kotha, C.N. Dewey, C. Ané

BUCKy: gene tree/species tree reconciliation with Bayesian concordance analysis

Bioinformatics, 26 (2010), pp. 2910-2911

[Crossref ↗](#) [View in Scopus ↗](#) [Google Scholar ↗](#)

[Loss-Oliveira et al., 2016](#) L. Loss-Oliveira, C. Sakuragui, M.L. Soares, C.G. Schrago

Evolution of *Philodendron* (Araceae) species in Neotropical biomes

PeerJ, 4 (2016), p. e1744

[Crossref ↗](#) [View in Scopus ↗](#) [Google Scholar ↗](#)

[Luo et al., 2010](#) A. Luo, H. Qiao, Y. Zhang, W. Shi, S.Y.W. Ho, W. Xu, A. Zhang, C. Zhu

Performance of criteria for selecting evolutionary models in phylogenetics: a comprehensive study based on simulated datasets

BMC Evol. Biol., 10 (2010), pp. 1-13

[Google Scholar ↗](#)

[Mayo, 1986](#) Mayo, S.J., 1986. Systematics of *Philodendron* Schott (Araceae) with special reference to inflorescence characters. PhD Thesis, University of Reading, Reading, United Kingdom.

[Google Scholar ↗](#)

[Mayo, 1988](#) S.J. Mayo

Aspectos da evolução e da geografia do gênero *Philodendron* Schott (Araceae)

Acta Bot. Bras., 1 (1988), pp. 27-40

[Google Scholar ↗](#)

[Mayo, 1990](#) S.J. Mayo

History and infrageneric nomenclature of *Philodendron* (Araceae)

Kew Bull., 45 (1990), pp. 37-71

[Crossref ↗](#) [Google Scholar ↗](#)

[Mayo, 1991](#) S.J. Mayo

A revision of *Philodendron* subgenus *Meconostigma* (Araceae)

Kew Bull., 46 (1991), pp. 601-681

[Crossref ↗](#) [Google Scholar ↗](#)

[Mayo et al., 1997](#) S.J. Mayo, J. Bogner, P.C. Boyce

The Genera of Araceae

Royal Botanic Gardens, Kew, Richmond (1997)

[Google Scholar ↗](#)

[Michaels et al., 1994](#) S.D. Michaels, M.C. John, R.M. Amasino

Removal of polysaccharides from plant DNA by ethanol precipitation

Biotechniques, 17 (1994), pp. 274-276

[View in Scopus ↗](#) [Google Scholar ↗](#)

[Nagy et al., 2012](#) L.G. Nagy, S. Kocsubé, Z. Csanádi, G.M. Kovács, T. Petkovits, C. Vágvölgyi, T. Papp
Re-mind the gap! Insertion-deletion data reveal neglected phylogenetic potential of the nuclear ribosomal internal transcribed spacer (ITS) of Fungi
Plos One, 7 (2012), p. e49794

[Crossref ↗](#) [View in Scopus ↗](#) [Google Scholar ↗](#)

[Oliveira et al., 2014](#) L.L. Oliveira, L.S.B. Calazans, E.B. Morais, S.J. Mayo, C.G. Schrago, C.M. Sakuragui
Floral evolution of *Philodendron* subgenus *Meconostigma* (Araceae)
Plos One, 9 (2014), p. e89701

[Google Scholar ↗](#)

[Ripplinger and Sullivan, 2008](#) J. Ripplinger, J. Sullivan
Does choice in model selection affect maximum likelihood analysis?
Syst. Biol., 57 (2008), pp. 76-85

[Crossref ↗](#) [View in Scopus ↗](#) [Google Scholar ↗](#)

[Rogstad, 1992](#) S.H. Rogstad
Saturated NaCl-CTAB solution as a means of field preservation of leaves for DNA analyses
Taxon, 41 (1992), pp. 701-708

[Crossref ↗](#) [Google Scholar ↗](#)

[Ronquist et al., 2012](#) F. Ronquist, M. Teslenko, P. van der Mark, D.L. Ayres, A. Darling, S. Höhna, B. Larget, L. Liu, M.A. Suchard, J.P. Huelsenbeck
MrBayes 3.2: efficient Bayesian phylogenetic inference and model choice across a large model space
Syst. Biol., 61 (2012), pp. 539-542

[Crossref ↗](#) [Google Scholar ↗](#)

[Sakuragui, 2012](#) C.M. Sakuragui
Two new species and a revised key for *Philodendron* section *Schizophyllum* (Araceae)
Syst. Bot., 37 (2012), pp. 43-47

[Crossref ↗](#) [View in Scopus ↗](#) [Google Scholar ↗](#)

[Sakuragui et al., 2005](#) C.M. Sakuragui, S.J. Mayo, D.C. Zappi
Taxonomic revision of Brazilian species of *Philodendron* section *Macrobelyium*
Kew Bull., 60 (2005), pp. 465-513

[View in Scopus ↗](#) [Google Scholar ↗](#)

[Sakuragui et al., 2018](#) C.M. Sakuragui, L.S.B. Calazans, L.L. Oliveira, E.B. Morais, A.M. Benko-Iseppon, S. Vasconcelos, C.E.G. Schrago, S.J. Mayo

Recognition of the genus *Thaumatophyllum* Schott – formerly *Philodendron* subg. *Meconostigma* (Araceae) – based on molecular and morphological evidence

PhytoKeys, 98 (2018), pp. 51-71

[Crossref ↗](#) [View in Scopus ↗](#) [Google Scholar ↗](#)

[Shaw et al., 2007](#) J. Shaw, E.B. Lickey, E.E. Schilling, R.L. Small

Comparison of whole chloroplast genome sequences to choose noncoding regions for phylogenetic studies in angiosperms: the tortoise and the hare III

Am. J. Bot., 94 (2007), pp. 275-288

[Crossref ↗](#) [View in Scopus ↗](#) [Google Scholar ↗](#)

[Stamatakis, 2014](#) A. Stamatakis

RAxML Version 8: a tool for phylogenetic analysis and post-analysis of large phylogenies

Bioinformatics, 30 (2014), pp. 1312-1313

[Crossref ↗](#) [Google Scholar ↗](#)

[The Plant List, 2013](#) The Plant List, 2013. Version 1.1. <http://www.theplantlist.org> ↗. (accessed 10 December 2017).

[Google Scholar ↗](#)

[Weising et al., 2005](#) K. Weising, H. Nybom, K. Wolff, G. Kahl

DNA Fingerprinting in Plants, Principles, Methods, and Applications (second ed.), CRC Press, Boca Raton (2005)

[Google Scholar ↗](#)

[Wong et al., 2013](#) S.Y. Wong, P.J. Tan, K.K.W. Ng, A.S. Othman, H.B. Lee, F.B. Ahmad, P.C. Boyce

Phylogeny of Asian *Homalomena* (Araceae) based on the ITS region combined with morphological and chemical data

Syst. Bot., 38 (2013), pp. 589-599

[View in Scopus ↗](#) [Google Scholar ↗](#)

[Wong et al., 2016](#) S.Y. Wong, A.W. Meerow, T.B. Croat

Resurrection and new species of the Neotropical genus *Adelonema* (Araceae: *Philodendron* Clade)

Syst. Bot., 41 (2016), pp. 32-48

[Google Scholar ↗](#)

Zotz, 2013 G. Zotz

'Hemiepiphyte': a confusing term and its history

Ann. Bot., 111 (2013), pp. 1015-1020

[Crossref ↗](#) [View in Scopus ↗](#) [Google Scholar ↗](#)

Cited by (12)

[Hemiepiphytes revisited](#)

2021, Perspectives in Plant Ecology, Evolution and Systematics

Citation Excerpt :

...At the crown node of subgenus *Meconostigma*, a shift from climbing to self-supporting terrestrial occurred, corresponding to the prevailing habit in this lineage. In a study with a broader sampling of subgenus *Meconostigma*, however, the heliophilous hemiepiphytes *P. goeldii*, *P. solimoesense*, and *P. venezuelense* – all from the northern Amazon basin – represent the basal lineages within the subgenus (Vasconcelos et al., 2018). Thus, the terrestrial and saxicolous species (including some facultative hemiepiphytes) from open habitats in eastern Brazil may have evolved from hemiepiphytic ancestors from Amazonian rainforests....

[Show abstract](#) ✓

[Cytomolecular diversity among *Vigna* Savi \(Leguminosae\) subgenera ↗](#)

2024, Protoplasma

[Target sequence data shed new light on the infrafamilial classification of Araceae](#)

↗

2023, American Journal of Botany

[*Philodendron josephii* \(Araceae\), a new species from central Amazonia, Brazil ↗](#)

2023, Phytotaxa

[Taxonomic Novelties in *Philodendron* subg. *Philodendron* \(Araceae\) from Panama](#)

↗

2022, Novon

Unraveling the plant diversity of the Amazonian canga through DNA barcoding ↗

2021, Ecology and Evolution



[View all citing articles on Scopus ↗](#)

© 2018 Elsevier Inc.



All content on this site: Copyright © 2024 Elsevier B.V., its licensors, and contributors. All rights are reserved, including those for text and data mining, AI training, and similar technologies. For all open access content, the Creative Commons licensing terms apply.

